

Estimation of First-Year Sea Ice Thickness with Seafloor Distributed Acoustic Sensing

Michael G. Baker, Robert E. Abbott
Sandia National Laboratories, Geophysics Department



Abstract

Monitoring programs for sea ice thickness currently rely on estimations of freeboard height collected by satellite-based instrumentation; however, these methods provide only kilometer-scale resolution and suffer blackout dates based on cloud cover or available daylight. Using one week of data collected during April 2022 with the first ever deployment of distributed acoustic sensing (DAS) to an ice-covered seafloor, we demonstrate that the dispersion of wind-driven flexural-gravity waves may be inverted to provide estimates of sea ice thickness. We show that coherent and persistent short-to-mid period (3–20 s) wave trains observed by the seafloor DAS have dispersion relationships consistent with flexural-gravity waves traveling within the sea ice and coupling to the sea floor via hydrostatic pressure. Wind-driven flexural-gravity waves have a frequency-dependent activation wind speed which we exploit to construct empirical dispersion curves for each channel along the cable. Using a simple grid search we then estimate ice thickness by minimizing the misfit between observed and predicted flexural-gravity wave dispersion curves. This method has potential for site-specific monitoring of sea ice at spatial and temporal resolutions greatly exceeding those of satellite-based methods.

Instrumentation

We interrogated an existing telecommunications fiber optic cable (owned by Quintillion) extending into the Beaufort Sea from Oliktok Point, Alaska (Figure 1). The cable is direct-buried in a trench 2 m below the seafloor and contains large-diameter, transoceanic fiber (Corning Vascade EX2000). An optical amplifier at ~ 42 km places a hard-limit on DAS range.

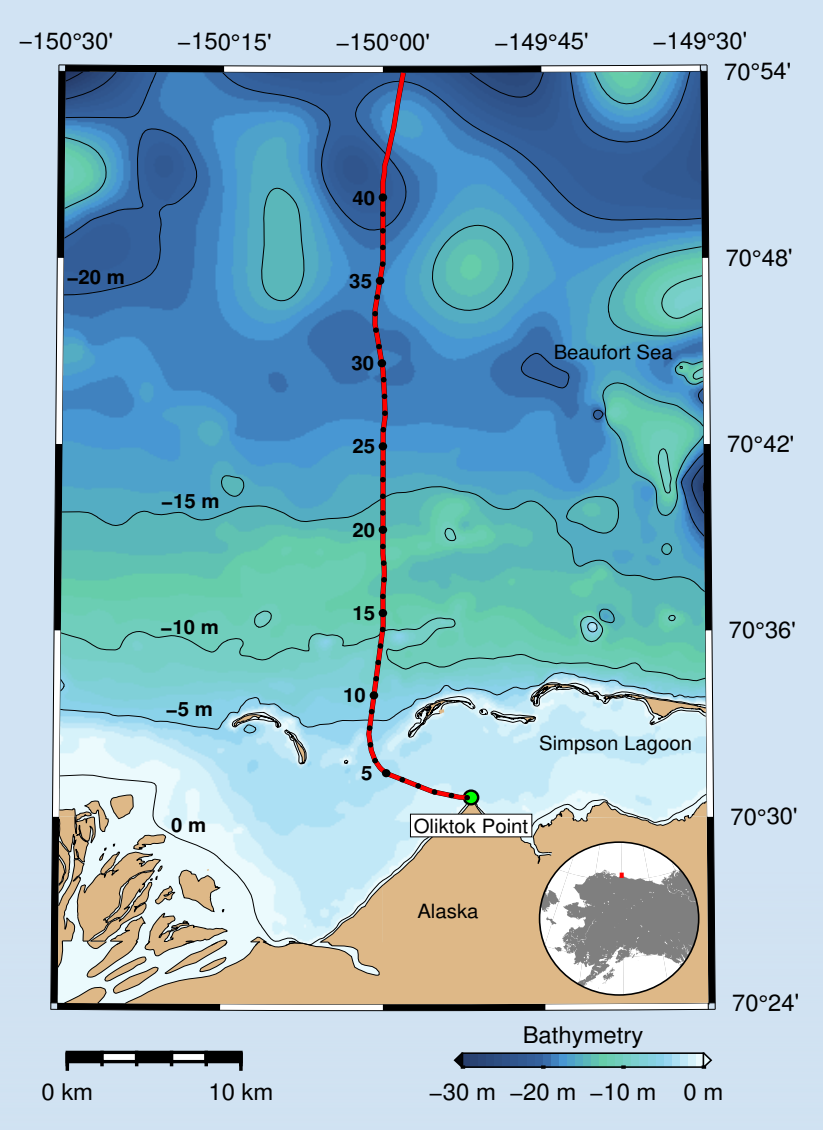


Figure 1. Cable map.

We recorded four one-week campaigns during each of 2021 and 2022, targeting a representative period of the annual sea ice cycle: ice-bound, breakup, ice-free, and freezing. The analysis discussed here uses ice-bound data recorded in April, 2022.

DAS signal-to-noise from the fiber optic cable was sufficient to record out to 37.4 km. We used a Silixa iDAS™ set for 2 m spatial resolution and 1000 Hz sample rate; gauge length was 10 m. With these parameters, we collected 3.1 TB of data per day, for an approximate total of 160 TB.

Background Theory

Flexural-gravity (FG) waves are a form of asymmetric Lamb waves that occur in floating elastic plates, wherein the restoring force is provided by a frequency-dependent combination of plate elasticity and buoyancy (Ewing & Crary, 1934). FG waves in sea ice may be caused by the collision of ocean gravity waves with the ice front, or by surface-parallel tractions imposed by wind (Figure 3).

FG waves are dispersive and dependent on ice thickness and water column depth. Wind-driven FG waves may occur only when wind speed is equal to or greater than FG wave speed; this activation wind speed may therefore be exploited to construct an empirical estimation of a snow- and ice-thickness-dependent dispersion curve, given known water column depths and assumed ice elastic parameters.

Data

We use DAS-measured strain-rate recorded from 2022-04-08 1100 through 2022-04-09 1700 UTC. During this period, wind speed monotonically increased and then decreased through a range of 0–12 m/s (Figure 2). Wind speed was measured with an ad hoc, in situ weather station sited next to the cable termination building at Oliktok Point.

We use data recorded only between 0.5 and 11.0 km along-fiber distance. At distances less than 0.5 km, the cable is decoupled from ground strain due to its placement inside an air- and water-filled conduit. At distances greater than 10.5 km, the water column depth pushes the FG wave dispersion curve to higher activation wind speeds than we observed. (Figure 2).

We decimate to 10 Hz resolution to reduce processing time.

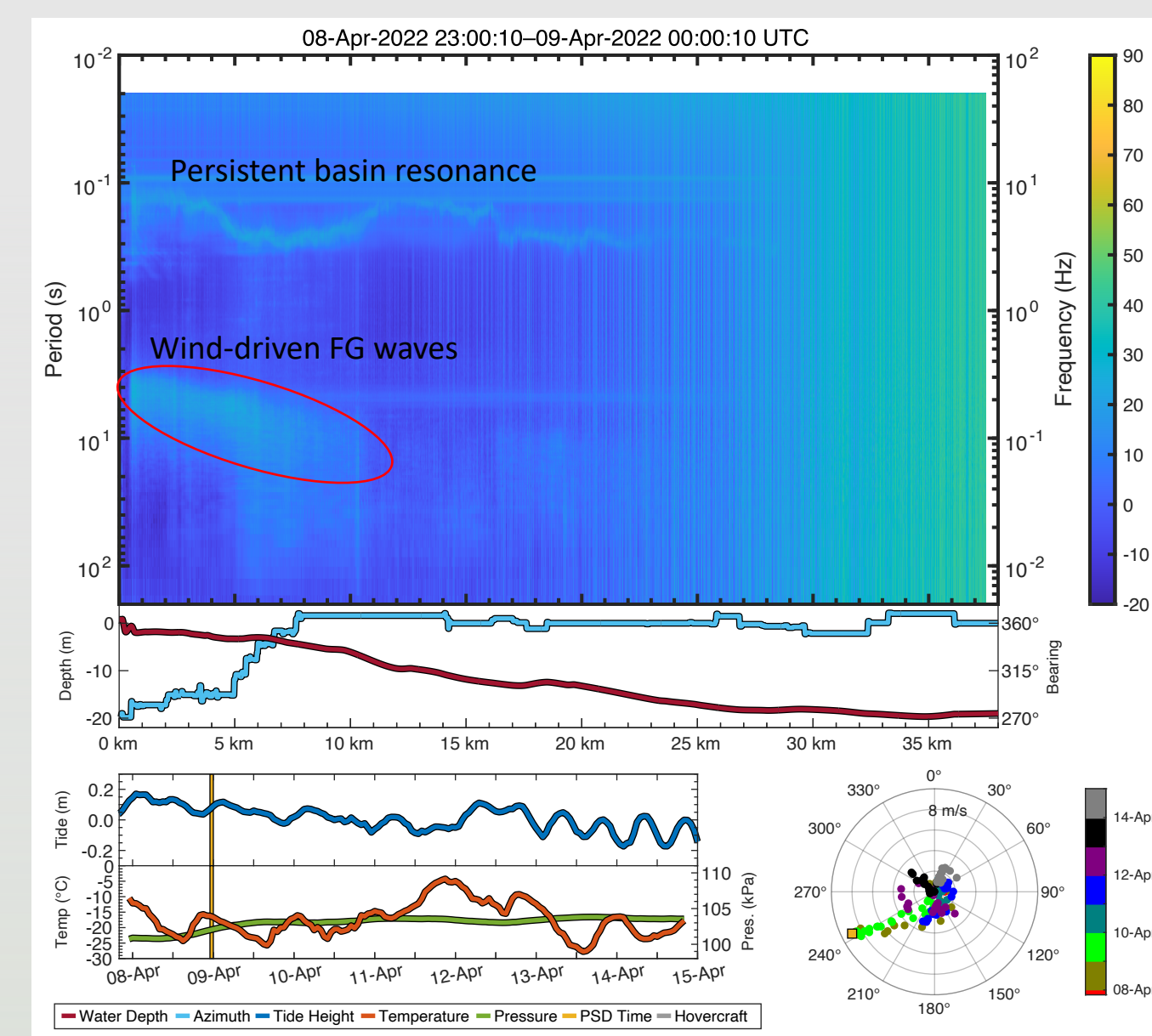


Figure 2. Example DAS power spectral density versus along-fiber distance for an hour of data recorded coincident with maximum wind speeds (lower right).

Method

For each channel:

- 1) Apply a suite of Ricker filters centered at 3–20 s in 0.5 s increments.
- 2) Calculate RMS time series using 60 s causal windows.
- 3) Create a histogram of observed wind speed vs period-band RMS.
- 4) Calculate the median observed RMS at each period and wind speed (Figure 4).
- 5) Create a suite of flexural-gravity wave dispersion curves across a grid of snow and ice thickness values (Table 1). Water column depth is fixed based on channel-specific interpolated depths, corrected for tide height (Figure 2).
- 6) Calculate line integrals through period-wind speed space to find the largest magnitude dispersion curve (Figure 4).
- 7) Calculate the snow & ice thickness as the weighted mean of the 95th percentile of dispersion curve fit values (Figure 5).

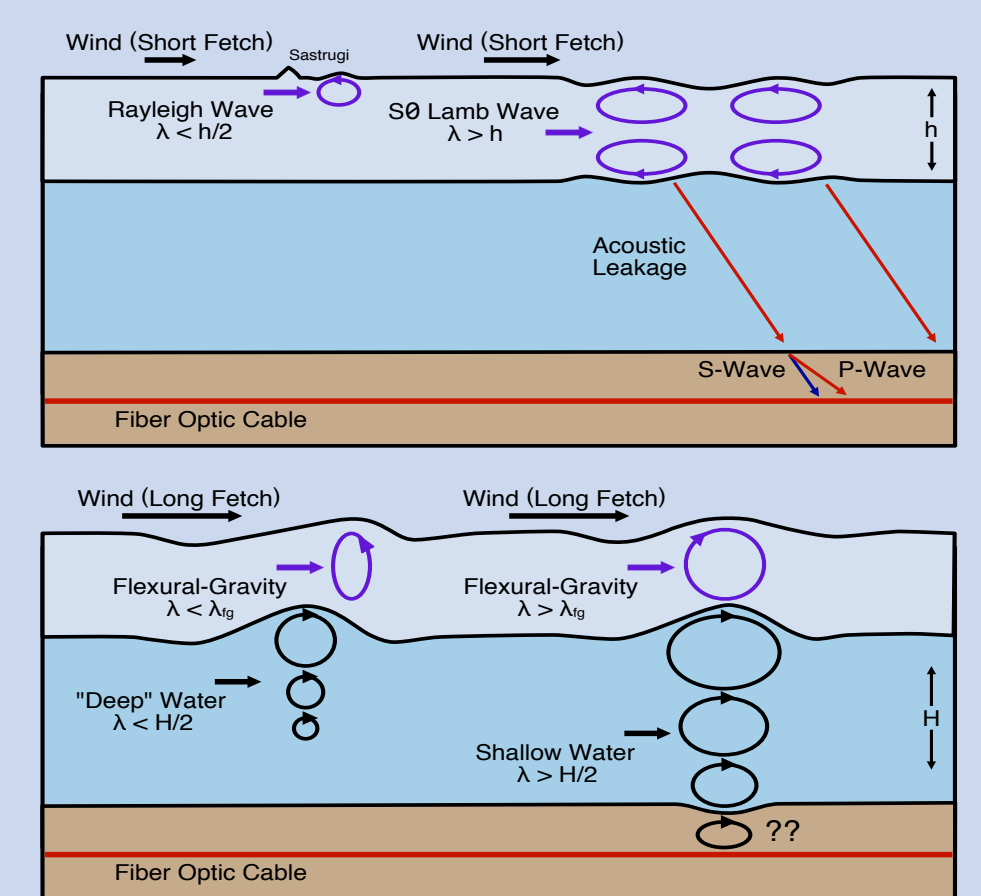


Figure 3. Schematic (not to scale) of floating ice wave modes and their potential for observation by a seafloor DAS. FG waves shown at bottom.

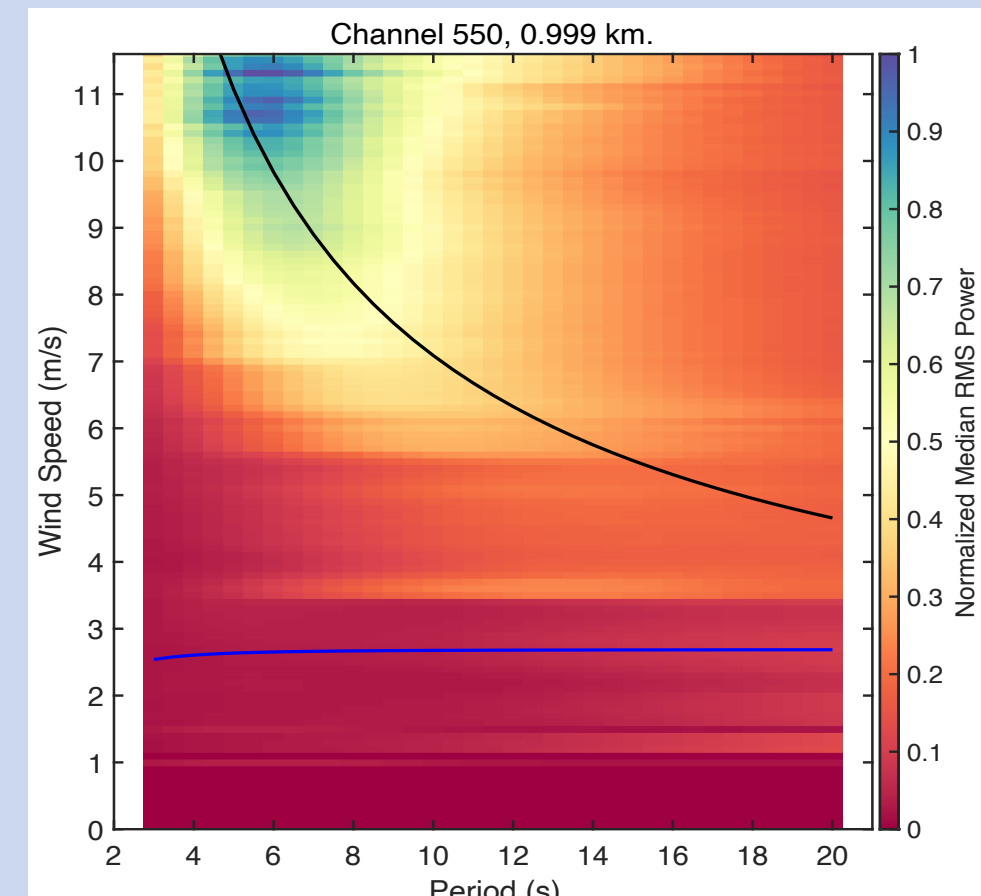


Figure 4. DAS RMS values for an example channel. Black curve is the best-fit FG dispersion curve.

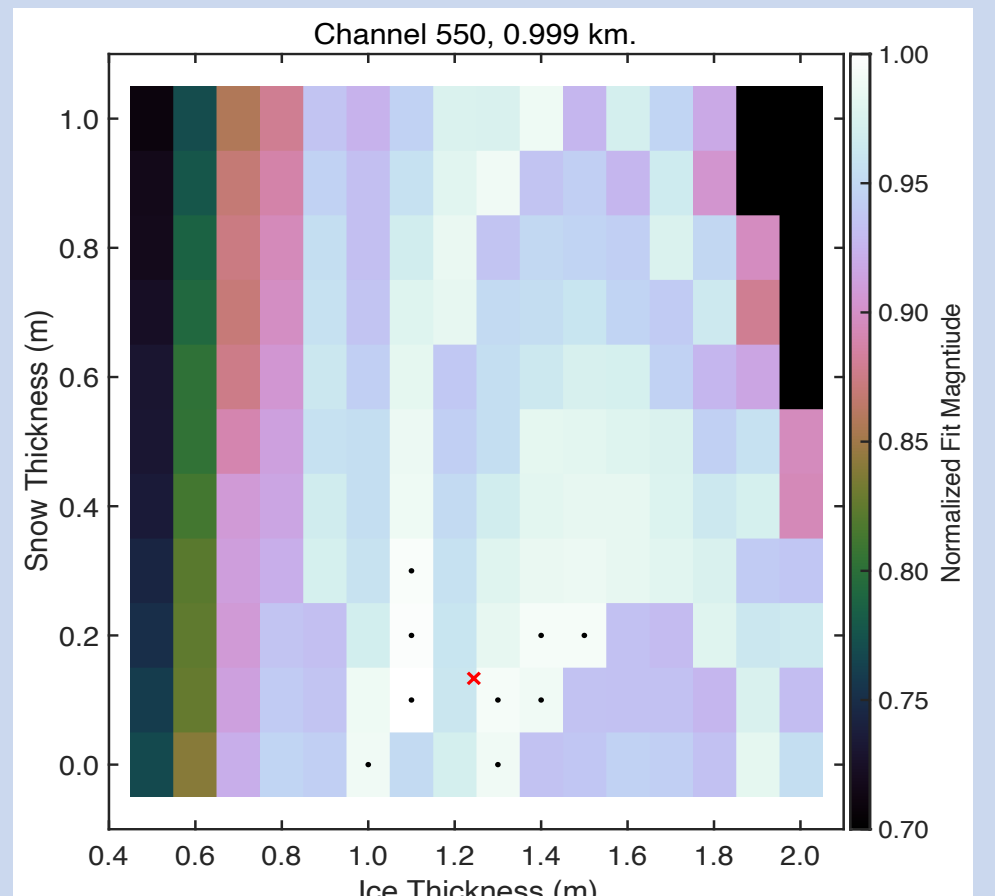


Figure 5. Example grid search results for FG dispersion curve fitting. Red X is the weighted mean of the 95th percentile (black dots).

Results

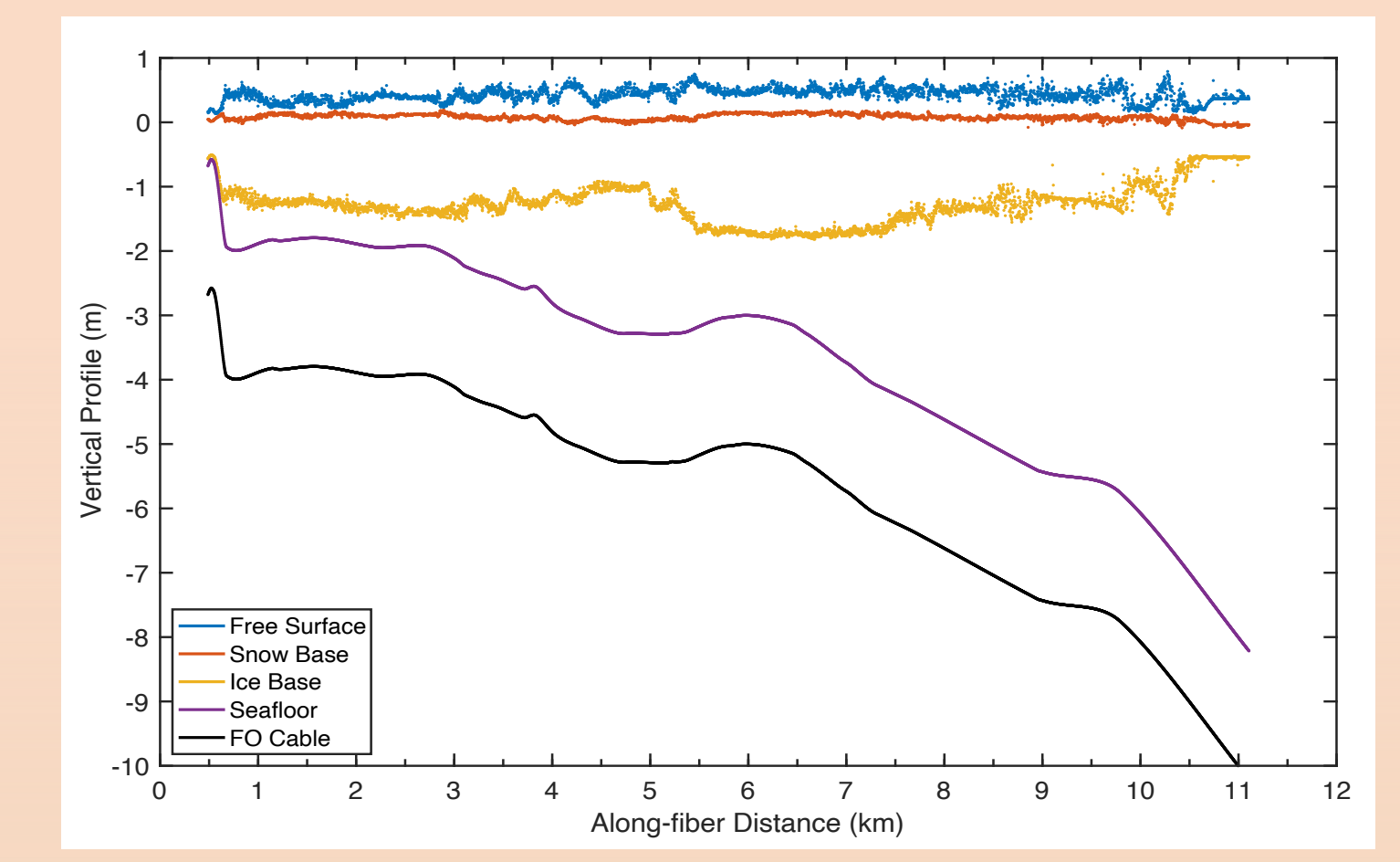


Figure 6. Profile of inverted ice and snow thicknesses, accounting for buoyancy. Horizons have not been laterally smoothed.

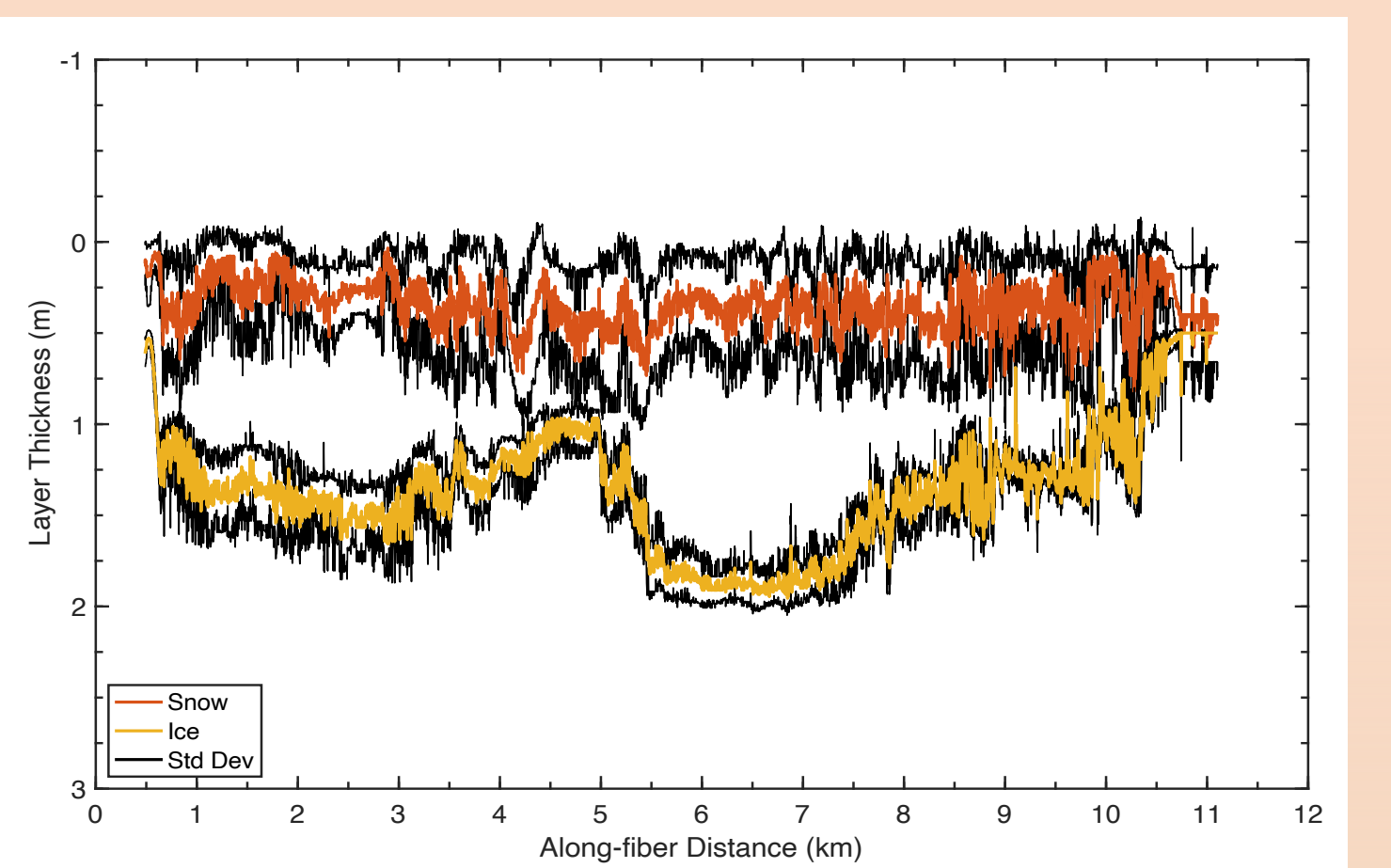


Figure 7. Inverted ice and snow thicknesses with weighted standard deviations. Buoyance offsets have not been incorporated.

Discussion

The lateral continuity of ice layer thickness gives credibility to the efficacy of the dispersion curve extraction algorithm. The larger variance in snow layer thickness is due to the smaller contribution of the snow layer to the FG wave solution. A total thickness of ~ 1.5 m is comparable to satellite-based measurements. Future research efforts will focus on ground truthing of ice thickness and elastic parameters, and quantification of the error induced by tidal variations in water column depth.